Adaptation of microbial resource allocation affects modeled long term soil organic matter and nutrient cycling.

Thomas Wutzler[1], **Marion Schrumpf**[1], **Bernhard Ahrens**[1], **Söhnke Zähle**[1], **and Markus Reichstein**[1]

[1]Max Planck Institute for Biogeochemistry, Hans-Knöll-Straße 10, 07745 Jena, Germany

Correspondence to: Thomas Wutzler
(twutz@bgc-jena.mpg.de)

Abstract. necessary to understand C and N use efficiencies of microbial soil organic matter (SOM) decomposers. While important controls of those efficiencies by microbial community adaptations have been shown at pore scale, an abstract simplified representation of community adaptations is needed at ecosystem scale. Therefore we developed the soil extracellular enzyme allocation model (SEAM) that described C and N dynamics at ecosystem and decadal scale. We explicitely modeled several alternative community adaptation strategies of resource allocation to extracellular enzymes and enzyme limitations on SOM decomposition. Using SEAM, we explored the effects of those alternative strategy-hypotheses on SOM and inorganic N cycling. Simulations showed that the revenue enzyme allocation strategy was most competitive, which accounted for adaptations to both, stoichiometry and amount of different SOM resources. Predictions of the holistic SEAM model were qualitatively similar to microbial group explicit models with the ability to represent priming effects, and the buildup or decline of SOM pools depending on inorganic N inputs. We found that soil enzyme allocation strategies strongly affect long term soil organic matter cycling and nutrient recycling. The findings imply that ecosystem scale models should account for adaptation of C and N use efficiencies to represent and understand C-N couplings. The combination of stoichiometry and optimality principles is a promising route to yield simple formulations of such adaptations at community level suitable for incorporation into land surface models.

1 Introduction

The global element cycles of carbon (C) and nitrogen (N) are intrically linked and cannot be understood without their interactions (Thornton et al., 2007; Janssens et al., 2010; Zaehle and Dalmonech, 2011). The links between nutrient cycles are especially strong in the dynamics of soil organic matter (SOM) because all of the SOM has to be depolymerized and successively mineralized by a microbial community with a rather strict homeostatic regulation (Sterner and Elser, 2002; Zechmeister-Boltenstern et al., 2015).

Faced with imbalances between stoichiometry of OM, i.e. the litter and SOM they feed on, and stoichiometric requirements of decomposers, decomposers have three options (Mooshammer et al., 2014b). First, they can adapt their carbon use efficiency (CUE) or nutrient use efficiency (NUE) (Sinsabaugh et al., 2013). The alteration of CUE has shown to have large consequences on prediction of carbon sequestration in SOM (Allison, 2014; Wieder et al., 2013). Regulation of NUE has consequences for nutrient recycling and loss of nutrients from the ecosystem (Mooshammer et al., 2014a) and soil plant feedback (Rastetter, 2011). As a second option, decomposer communities can adapt their stoichiometric requirements. Community composition can shift between species with high C/N ratio, such as many fungi, or species with lower C/N ratio, such as many bacteria (Cleveland and Liptzin, 2007; Xu et al., 2013), although the flexibility is very narrow. As a third option, decomposers can adapt their allocation of resources into production of different extracellular enzymes to preferentially degrade fractions of SOM that differ by their stoichiometry (Moorhead et al., 2012).

Representation and consequences of stoichiometry on element cycling differ between models at different scales. Most soil models at ecosystem scale employ the first option and

use CUE or NUE to represent stoichiometric controls on respiration and mineralization fluxes (Manzoni et al., 2008). However, modelling studies at the pore scale, which is relevant to microbes, show the important effect of community adaptation and their emerging effects on element cycling (Allison and Vitousek, 2005; Resat et al., 2011; Wang et al., 2013). Competition among several microbial groups that differed in expression of different enzymes resulted in a simulated approximately equally high CUE across a wider range of litter stoichiometry (Kaiser et al., 2014). Hence, there is a need to capture the effects of community adaptation also in models at ecosystem scale.

Effects of microbial diversity can be represented at ecosystem scale by at least two options. First, competition of several microbial populations can be explicitely modeled to represent stoichiometric effects such as sustained sequestration of N with high N inputs (Perveen et al., 2014). Second, adaptation of effective properties of the entire microbial community, such as uptake efforts (Rastetter et al., 1997; Rastetter, 2011), can represent the emerging effects in an abstract but dynamic and adaptive way.

The adaptation of enzyme production was recently formalized by the conceptual EEZY model (Moorhead et al., 2012). While this model showed the principle feasibility of this strategy in short term, it did not implement feedback to SOM pools and therefore could not study consequences for longer term SOM cycling.

Out task, therefore, was to tackle the need of capturing the effects of adaptive enzyme production on long term SOM dynamics and nutrient recycling. We extended the EEZY model to explore different consequences of alternative enzyme allocation schemes.

This paper first introduces the SEAM model (Section 2.1), a dynamical model of SOM cycling that explicitly represents microbial strategies (Section 2.3) of producing several extracellular enzyme pools. Next, the effects of those strategies on SOM cycling are presented by prototypical examples (Sections 2.4 and 3.1). Finally, a calibration to an intensive pasture site (Section 2.5) demonstrates the usability of the model (Section 3.2) and compares its predictions to the ones of the Symphony model (Perveen et al., 2014), which explicitely models several microbial-group.

This study shows that different decomposer enzyme allocation strategies have large consequences on long term SOM dynamics and nutrient recycling. It proposes a holistic scheme to represent effects of microbial adaptation of enzyme production on SOM cycle at the ecosystem scale.

2 Methods

2.1 Soil Enzyme Allocation Model (SEAM)

Development of the dynamic Soil Enzyme Allocation Model (SEAM) allowed to explore consequences of enzyme allocation strategies for SOM cycling at the soil core scale. The

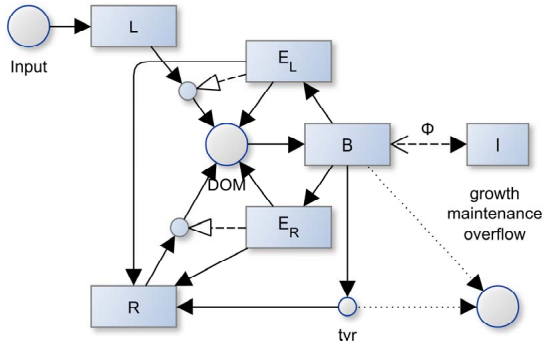

Figure 1. Model structure of SEAM: Two resource pools (L and R) which differ in their elemental ratios are depolymerized by respective enzymes (E_L and E_R). The simple organic compounds (DOM) are taken up by the microbial community and used for synthesizing new biomass (B), new enzymes, for catabolic respiration. Stoichiometric imbalance between DOM and B causes overflow respiration or mineralization/immobilization (Φ_B) of inorganic N (I), which is detailed Fig. 2. Boxes correspond to pools, black arrow heads to mass fluxes, white arrow heads to other controls, and disks represent partitioning of fluxes. Solid lines represent fluxes of both C and N, while dotted and dashed lines represent separate C or N fluxes respectively.

modelled system are C and N pools in SOM in a representative elemental volume of soil. The system could be soil of a laboratory incubation or a layer of a soil profile, e.g. its upper 20cm. The model represents different pools of C and N as state variables and specifies dynamic equations for the mass fluxes. It is driven by inputs of plant litter (both above ground and rhizodeposition) and inorganic N inputs, as well as prescribed uptake of inorganic N by roots. It computes output fluxes of heterotrophic respiration and leaching of inorganic N.

Key features are first, the representation of several SOM pools that differ by their stoichiometry, i.e. elemental ratios, and second, the representation of specific enzymes that degrade those SOM pools. The quality spectrum is modelled by two classes: a C rich litter pool, L, and a N rich pool that consists mainly of microbial residues, R (Fig. 1).

The most important assumptions are described in the following paragraphs, while the symbols are explained in Tab. 1 and detailed model equations are given in Appendix A.

Table 1. Model parameters and drivers. The two value columns refer to the prototypical example and the grassland calibration respectively.

Symbol	Definition	Value		Unit	Rational
State variables					
L	C in litter		571	gm^{-2}	quasi steady state
L_N	N in litter		8.15	gm^{-2}	(Perveen et al., 2014) (by their N/C ratio β)
R	C in residue substrate		10500	gm^{-2}	(Allard et al., 2007) (total stocks - L - dR)
R_N	N in residue substrate		968	gm^{-2}	by C/N ratio in (Perveen et al., 2014)
E_L	C in enzymes targeting L		0.34	gm^{-2}	quasi steady state
E_R	C in enzymes targeting R		0.20	gm^{-2}	quasi steady state
B	microbial biomass C		89.2	gm^{-2}	quasi steady state
I	inorganic N		2.09	gm^{-2}	(Perveen et al., 2014)
Model parameters					
β_B	C/N ratio of microbial biomass	11	11	gg^{-1}	(Perveen et al., 2014)
β_E	C/N ratio of extracellular enzymes	3.1	3.1	gg^{-1}	(Sterner and Elser, 2002)
β_{input_L}	C/N ratio of plant litter inputs	30	70	gg^{-1}	(Perveen et al., 2014) $(1/\beta)$
k_R	maximum decomposition rate of R	1	4.39e-2	yr^{-1}	calibrated
k_L	maximum decomposition rate of L	5	1.95	yr^{-1}	calibrated
k_N	enzyme turnover rate	60	60	yr^{-1}	(Burns et al., 2013)
k_{NB}	enzyme turnover entering DOM rather than R	0.8	0.8	(-)	mostly small proteins
a_E	enzyme production per microbial biomass	0.365	0.365	yr^{-1}	$\approx 6\%$ of biomass synthesis
K_M	enzyme half saturation constant	0.05	0.05	gm^{-2}	magnitude of DOC concentration
τ	microbial biomass turnover rate	6.17	6.17	yr^{-1}	(Perveen et al., 2014) $(s/\epsilon_{\mathrm{tvr}})$
m	specific rate of maintenance respiration	1.825	0	yr^{-1}	(van Bodegom, 2007), zero in (Perveen et al., 2014)
ϵ	anabolic microbial C substrate efficiency	0.5	0.53	(-)	calibrated
ν	aggregated microbial organic N use efficiency	0.7	0.9	(-)	(Manzoni et al., 2008)
ϵ_{tvr}	microbial turnover that is not mineralized	0.3	0.8	(-)	part of turnover is consumed by predators
i_B	maximum microbial uptake rate of inorganic N	25	25	yr^{-1}	larger than simulated immobilization flux
l	inorganic N leaching rate	-	0.959	yr^{-1}	(Perveen et al., 2014) (l)
Model drivers, i.e. fluxes across system boundary					
input_L	litter C input		969.16	$\mathrm{gm}^2\mathrm{yr}^{-1}$	(Perveen et al., 2014) $(m_p C_p^{obs})$
i_I	inorganic N input		22.91	$\mathrm{gm}^2\mathrm{yr}^{-1}$	(Perveen et al., 2014)
k_{IP}	inorganic plant N uptake		16.04	$\mathrm{gm}^2\mathrm{yr}^{-1}$	(Perveen et al., 2014) (assuming plant steady state: plant N export + litter N input)
Fluxes and quantities derived within the system					
α	proportion of enzyme investments allocated to production of E_R			(-)	
syn_B	C for microbial biomass synthesis			$\mathrm{gm}^2\mathrm{yr}^{-1}$	
syn_E	C for enzyme synthesis			$\mathrm{gm}^2\mathrm{yr}^{-1}$	
tvr_B	microbial biomass turnover C			$\mathrm{gm}^2\mathrm{yr}^{-1}$	
tvr_E	enzyme turnover C			$\mathrm{gm}^2\mathrm{yr}^{-1}$	
dec_S	C in decomposition of resource S (S is L or R)			$\mathrm{gm}^2\mathrm{yr}^{-1}$	
u_C, u_N	microbial uptake of C and N			$\mathrm{gm}^2\mathrm{yr}^{-1}$	
$\Phi_u, \Phi_B, \Phi_{\mathrm{tvr}}$	N mineralization with microbial DOM uptake, stoichiometric imbalance, and turnover			$\mathrm{gm}^2\mathrm{yr}^{-1}$	see Fig. 2

Decomposition of litter and residue pool follows an inverse Michaelis-Menten kinetics (Schimel and Weintraub, 2003), which is first order to the amount of OM, and saturating with the amount of the respective enzyme. C/N ratios, β, of the decomposition flux is equal to the C/N ratios of the decomposed pool. C/N ratios of biomass and enzymes are fixed while those of the resource pools may change over time due to changing C/N ratio of total influx to these pools. Imbalances in stoichiometry of uptake and microbial requirements are compensated by overflow respiration or N mineralization. Total enzyme allocation is a fixed fraction, a_E, of the microbial biomass, B, per time. But microbial community can use different strategies (Section 2.3) to adjust their allocation to production of alternative kinds of new enzymes. The DOM pool is assumed to be in quasi steady state and the sum of all influxes to the DOM pool, i.e. decomposition plus part of the enzyme turnover, is taken up by the microbial community. If expenses for maintenance and enzyme production cannot be met, the microbial biomass starves and declines.

2.2 Exchange with inorganic N pools

The imbalance flux, Φ_B, lets microbes mineralize access N or immobilize required N up to a maximum rate of $u_{\mathrm{imm,Pot}}$, which increases linearly with the inorganic N pool. While this stoichiometric imbalance flux is the most widely implemented flux between microbial biomass and the inorganic carbon pool in SOM models (Manzoni and Porporato, 2009), it is not sufficient to recycle N to the inorganic pool if microbial biomass is itself uptake N limited. Therefore, two additional mineralization fluxes are implemented with the SEAM model (Fig. 2). First, a fraction of microbial DON uptake, termed uptake mineralization Φ_u, is apparently mineralized that accounts for C-limited locations in heterogeneous soil (Manzoni et al., 2008). Second, a fraction of microbial turnover is mineralized that accounts for grazing. Grazers respire part of the grazed biomass C for their energy, and must release an equivalent amount of nutrients to match their stoichiometric demands. This mineralization component, here termed turnover mineralization Φ_{tvr}, has been formalized in the soil microbial loop hypothesis (Clarholm, 1985; Raynaud et al., 2006).

A refinement of the term N limitation (Table 2) is required by the introduction of the additional N mineralization fluxes. When microbes can meet their stoichiometric demand only by immobilizing N, we suggest the term uptake N limitation. When the immobilization flux cannot meet microbe's stoichiometric requirements, we suggest the term microbial N limitation. Despite the maximum immobilization flux there might still be a net mineralization due to uptake mineralization and turnover mineralization. When there is a net immobilization, i.e. a net transfer from inorganic pool to the organic pools of SOM and microbial biomass, we suggest the term SOM N limitation still searching for a better term here.

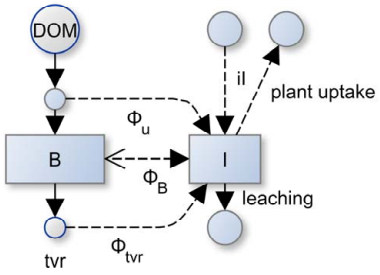

Figure 2. In addition to the maybe negative imbalance flux, Φ_B of microbial biomass, B, there are additional mineralization fluxes feeding the inorganic pool, I, due to mineralization during uptake, Φ_u, and mineralization during microbial turnover, Φ_{tvr}. The N dynamics depends also on fluxes across the system boundary, namely input of organic N with litter, input of inorganic N iI, leaching, and plant uptake of inorganic N.

Table 2. Increasing levels of N limitation

Term	Definition
Uptake N lim.	N in microbial uptake is less than constrained by other elements ($\Phi_B < 0$).
Microbial N lim.	Maximum immobilization flux is not enough to satisfy microbial N requirements ($-\Phi_B = u_{\mathrm{imm,Pot}}$).
SOM N lim.	There is a net transfer from the inorganic pool to the organic pools ($\Phi_B + \Phi_u + \Phi_{\mathrm{tvr}} < 0$).

2.3 Enzyme allocation strategies

Three different strategies of allocating investments among production of alternative enzymes were explored in this study (Table 3). Microbes allocate a proportion α of total enzyme investments, $a_e\, B$, to the production of enzymes targeting the N rich R resource and proportion $1-\alpha$ to the production of enzymes targeting the N poor but better degradable L resource: $\mathrm{alloc}_{E_R}/(\mathrm{alloc}_{E_R}+\mathrm{alloc}_{E_L}) = \alpha$.

The **Fixed** strategy assumes that allocation is independent and not changing with changes in substrate availability.

$$\alpha = \mathrm{const.} = 1/2 \tag{1}$$

This strategy corresponds to the models where decomposition rate is a function of microbial biomass (Wutzler and Reichstein, 2008).

The **Match** strategy assumes that microbes regulate enzymes production in a way that decomposition products balance their stoichiometric demands (Moorhead et al., 2012). The partitioning coefficient is derived by equating the C/N

Table 3. Microbial enzyme allocation strategies

Strategy	Allocation is
Fixed	independent, constant
Match	adjusted to achieve balanced growth ($\beta_{DOM} = \beta_B$)
Revenue	proportional to return per investments into enzymes

ratio of the sum of uptake fluxes after other expenses to the C/N ratio of microbial biomass, β_B.

$$\frac{\epsilon(\mathrm{dec}_L + \mathrm{dec}_R - r_M)}{\mathrm{dec}_L/\beta_L + \mathrm{dec}_R/\beta_R - \Phi_M} = \beta_B, \tag{2}$$

where dec_L, and dec_R are depolymerization fluxes of the litter and residue resources respectively, r_M is maintenance respiration, ϵ is the anabolic microbial efficiency (A7), and β_i are C/N ratios of the respective pools i, and Φ_M is the net flux of N from living microbes to the mineral N pool. Equation 2 for simplicity neglects the small inputs of enyzmes to DOM. Here, we assume that microbes use the maximal immobilization of inorganic N, $u_{\mathrm{imm,Pot}}$ (A9), to meet their stoichiometric requirements with the Match strategy. Hence, the net N flux is the difference between mineralization during uptake and the immobilization: $\Phi_M = \Phi_u - u_{\mathrm{imm,Pot}}$. With microbial N limitation, (2) has no solution, enzymes are allocated entirely to the N-rich resource ($\alpha = 1$), and excess carbon is respired by overflow respiration.

When the current sum of enzyme levels, E is assumed to be in quasi steady state for given amounts of resource and microbial biomass, then equation 2 can be solved for allocation partitioning, α, because the decompostion fluxes dec_L and dec_R are functions of α (Appendix B).

$$\alpha_M = f_{\alpha\mathrm{Fix}}(L, \beta_L, R, \beta_R, E_L, E_R, r_M, \Phi_M) \tag{3a}$$

$$\alpha = \begin{cases} 0, & \text{if} \alpha_M \leq 0 \\ 1, & \text{if} \alpha_M \geq 1 \\ \alpha_M, & \text{otherwise} \end{cases} \tag{3b}$$

The bound to one is necessary to handle the case of microbial N limitation, and the bound to zero corresponds to the theoretical case where the C rich resource may not suffice to cover microbial C demands. Function $f_{\alpha\mathrm{Fix}}$ is given in appendix B and the SYMPY script of its derivation is given with supplementary material.

The **Revenue** strategy assumes that microbial community adapts in a way so that investment into enzyme production is proportional to their revenue, i.e. their return per investment regarding the currently limiting element:

$$\alpha_C = \frac{\mathrm{rev}_{RC}}{\mathrm{rev}_{LC} + \mathrm{rev}_{RC}} \tag{4a}$$

$$\alpha_N = \frac{\mathrm{rev}_{RN}}{\mathrm{rev}_{LN} + \mathrm{rev}_{RN}}, \tag{4b}$$

Table 4. Prototypical simulation scenarios

Scenario	Explored issue
VarN-Incubation	Efficieny of using given fixed resource levels that vary by N content
Feedback-Steady	Possibility and size of steady state resource pools
Priming	Increased resource decomposition and mineralization after a pulse addition of fresh litter
CO_2-Fertilization	Continuous increase of litter C inputs but constant litter N inputs

where rev_S is the revenue from given resource S (S is either L or R) under C and N limitation respectively. The return is the current decomposition flux from the resource degraded by the respective enzyme, and the investment is assumed to be equal to enzyme turnover to keep current enzyme levels, E^*_S.

$$\mathrm{rev}_{SC} = \frac{\text{return}}{\text{investment}} = \frac{\mathrm{dec}_{S,Pot}\,\frac{E^*_S}{K_{M,S}+E^*_S}}{k_{NS}E^*_S} = \frac{\mathrm{dec}_{S,Pot}}{k_{NS}(K_{M,S}+E^*_S)} \tag{5a}$$

$$\mathrm{rev}_{SN} = \frac{\mathrm{dec}_{S,Pot}\,\frac{E^*_S}{K_{M,S}+E^*_S}/\beta_S}{k_{NS}E^*_S/\beta_E} = \mathrm{rev}_{SC}\,\frac{\beta_E}{\beta_S}, \tag{5b}$$

where k_{NS} is rate of enzyme turnover, $K_{M,S}$ is enzyme's resource affinity, $\mathrm{dec}_{S,Pot}$ is enzyme saturated decomposition flux (A4), and β are C/N ratios of the respective pools.

There are two resulting partitioning coefficients, α_C and α_N with C or N limited microbial biomass repectively. In order to avoid frequent large jumps under near co-limitation, SEAM implements a smooth transition between these two cases as a weighted average.

$$\alpha = \frac{w_{\mathrm{CLim}}\alpha_C + w_{\mathrm{NLim}}\alpha_N}{w_{\mathrm{CLim}} + w_{\mathrm{NLim}}}, \tag{6}$$

where w is the strength of the limitation of the respective element, specifically the ratio of required to available biomass synthesis fluxes (A13).

2.4 Prototypical simulation scenarios

Several prototypical simulation scenarios (Table 4) were used to explore consequences of different microbial enzyme allocation strategies for SOM dynamics. All scenarios used parameter values given in Table 1, if not stated specifically otherwise. Inorganic N pool was kept steady at $I = 0.4\mathrm{gN}$, here, while inorganic N feedback is studied in section 2.5.

The **VarN-Incubation** scenario explored how resources of given stoichiometry are used more or less efficiently for

microbial biomass growth with different enzyme allocation scenarios. It used a simplified model where all the inputs and feedback to the resource pools (L and R) and to the inorganic N pool (I) were neglected and these pools were kept constant ($dL/dt = dR/dt = 0$). It allowed microbes and enzyme levels to develop to a quasi steady state with the given resource supply. Hence, it simulated the end of a short term incubation where changes of litter and residue pools are negligible small. Specifically, it used fixed resource carbon of $L = 100\mathrm{gCm}^2$, $R = 400\mathrm{gCm}^2$. It set C/N ratio of the residue pool to $\beta_R = 7$, and varied the litter C/N ratio ($\beta_L = [18, .., 42]$).

The **Feedback-Steady** scenario explored the long term trajectories of the entire system including feedback to the substrate pools starting from a system state away from steady-state. Specifically, it set litter input to $\mathrm{input}_L = 400\ \mathrm{gCm}^2\mathrm{yr}^{-1}$ with C/N ratio $\beta_{\mathrm{input}_L} = 30$.

The **Priming** scenario explored the effect of rhizosphere priming, i.e the input of fresh litter into a bulk subsoil. It looked at the fluxes after an addition of $50gC$ carbon and a respective amount of N on a soil that otherwise received a litter input of only 30 $\mathrm{gCm}^2\mathrm{yr}^{-1}$ (and respective N) for a decade. It simulated a very easily degradable litter and amendmend, specifically with a maximum turnover of $k_L = 10\ \mathrm{day}^{-1}$.

The $\mathbf{CO_2}$**-Fertilization** scenario explored the effect of continuous increased carbon litter input that is expected with elevated atmospheric CO_2. It started from steady state for a litter input, applied 20% increased carbon inputs during years 10 to 60, and applied original carbon inputs again during the next 50 years. The N inputs were kept constant over time.

2.5 Calibration to a fertilized grassland site

To test the capability of the SEAM model to simulate the carbon sink of a grassland site, we calibrated the model using the revenue strategy to data of an intensive pasture. The model drivers and most of the parametrization was taken from the publication of (Perveen et al., 2014). The site is a temperate permanent grassland located at an altitude of 1040m in France (Laqueuille, 45°38'N, 2°44'E) and has an annual precipitation and temperature of 1200 mm and 7 °C, respectively.

The N balance of the fertilized grassland is characterized by high inorganic N-inputs. Part of this N is sequestered in accumulating SOM, part is leached and part is exported with plant biomass. In all scenarios, plant uptake of inorganic N was computed assuming the plants to be in steady state with the litter production and biomass exports.

Parameters were chosen corresponding to Table 1 in (Perveen et al., 2014). Three parameters were calibrated: the maximum decomposition rates of substrate pools, k_L and k_R, and the anabolic carbon use efficiency, ϵ. Initial pools were prescribed to observed values. Intial pools of microbial biomass and enzymes were set to the long-term state after a preliminary optimization in order to prevent large initial fluctuations. The calibrations used the *optim* function from R *stats* package (R Core Team, 2016) to minimize the differences between model predictions and observations normalized by the standard deviation of the observations. It used observations of the litter OM, the inorganic N, leaching, and rate of change of the total SOM pool ($\approx dR/dt$ if L is near quasis steady state). Next, the calibrated parameters were used generate predictions for scenarios of changed inputs to the system.

3 Results

First, the results of several prototypical artificial simulation scenarios clarify the general behaviour and features of the SEAM model. Next, results of a parameter calibration demonstrate the model's ability to simulate the observed C and N dynamics of an intensive pasture and explore feedbacks with the dynamics of the inorganic N pool.

3.1 Prototypical simulation scenarios

With the **VarN-Incubation** scenario, where the resource pools were fixed, there were differences among allocation strategies for the dependence of allocation α on the N content of the litter resource. The different strategies caused marked changes in biomass and imbalance fluxes (Fig. 3).

The Match strategy allowed balanced growth and efficient resource usage, but yielded less biomass than the other scenarios. When the litter contained enough N, microbes invested all resources into litter degrading enzymes. Across a wide range of litter C/N ratios (22 to 42) microbes did not need stoichiometric imbalance fluxes, i.e. mineralization of excess N or overflow respiration of excess C.

With the Revenue strategy enzyme allocation varied with litter N content, too. With litter containing enough N (low C/N ratio), still about 5% of the enzyme C expenditures were allocated into R degrading enzymes. This resulted in higher mineralization of excess N, but in turn allowed for a higher microbial biomass. With litter lacking enough N (higher C/N ratios), investment into R-degrading enzymes increased to about 30%, a value that was much lower than with the the Match strategy. Hence, the Revenue strategy yielded higher overflow respiration associated with low carbon use efficiency (CUE). However, at the same time, it yielded higher levels of microbial biomass.

The Fixed strategy yielded higher N-mineralization due to stoichiometric imbalance at low C/N ratios. At high C/N ratios its allocation was intermediate between the other strategies leading to intermediate values of all the other outputs.

With the **Feedback-Steady** scenario, where resource pools where refueled by microbial and enzyme turnover, both Fixed and the Revenue strategies caused resource pools to approach a steady state. However, the microbes with Match strategy solely degraded the stoichiometrically better match-

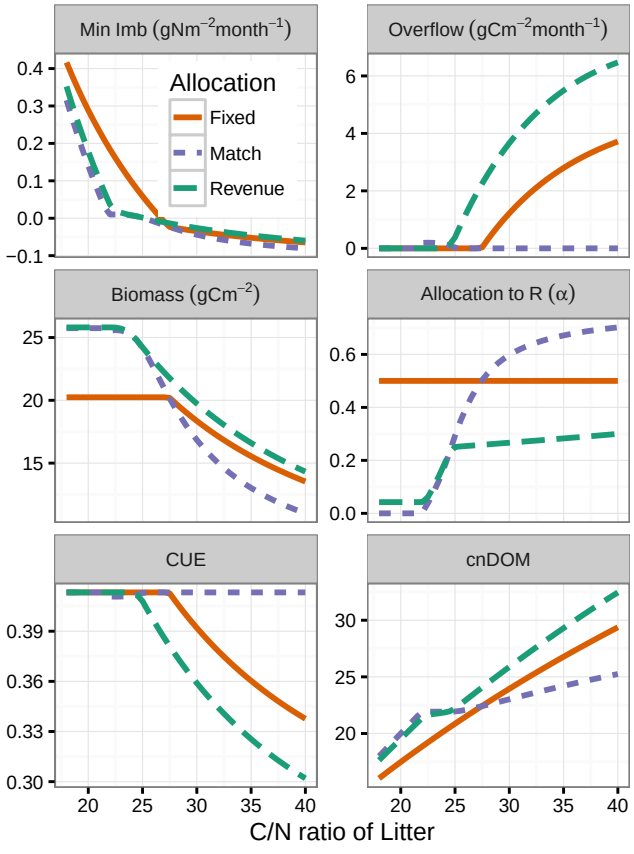

Figure 3. Match enzyme allocations strategy yielded highest resource efficiency, i.e. lowest mineralization fluxes at steady state with the VarN-scenario. Microbes with alternative strategies, however, competed better indicated by a higher biomass. Carbon use efficiency (CUE) and C/N ratio of the decomposition flux (cnDOM) helped to explain the different patterns.

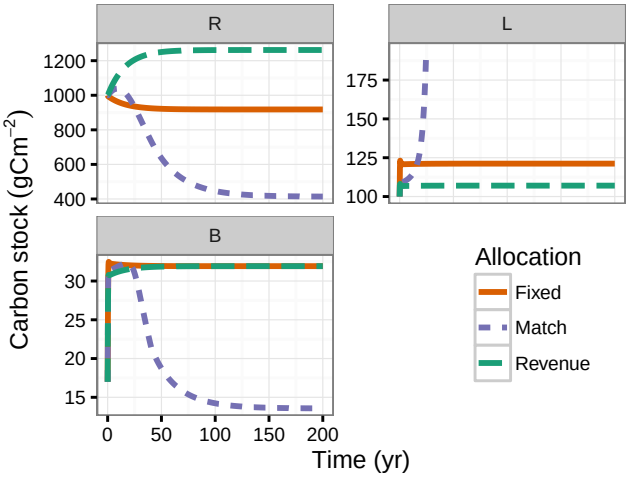

Figure 4. Match strategy was not viable when considering feedback to substrate pools with the SimSteady scenario, where microbes degraded a stoichiometrically matching but depleted R substrate pool.

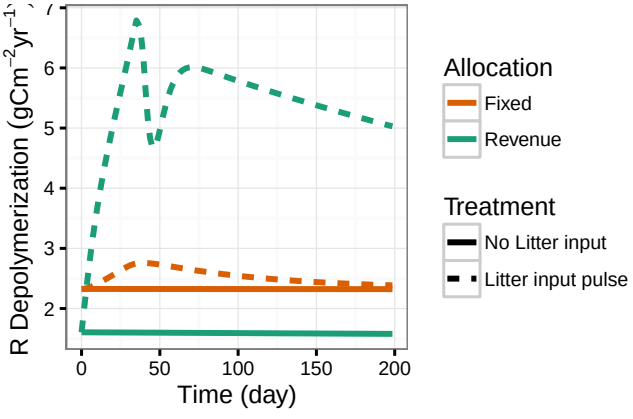

Figure 5. Residue depolymerization flux increased strongest with the Revenue strategy after amending a starved subsoil with a pulse of fresh litter with the Priming scenario.

ing high-N residue pool, R. Hence, they declined together with the R residues pool despite the large amount of N accumulating in the stoichiometrically less favourable litter pool (Fig. 4).

Because of the Match strategy was not able to simulate reasonable stocks when including feedback to resource pools in the model, it was omitted in the following simulation scenarios.

With the **Priming** scenario, where a soil was amended with a pulse of litter, a clear real priming effect was simulated. The priming effect is by a strongly enhanced decomposition of the residues pool (Fig. 5). It was stronger with the Revenue strategy than with the Fixed strategy. This stronger priming was mostly due to a higher microbial biomass with the Revenue strategy. Therefore also the N-mineralization flux due to microbial turnover was larger with the Revenue strategy (Fig. 6).

With the **CO_2-Fertilization** scenario, where litter C input was increased, enzyme allocation strategies yielded most marked differences between strategies in both SOM stocks (Fig. 7) and nutrient recycling (Fig. 8). While litter stocks L increased with both scenarios, the residues stock R slightly increased with the Fixed strategy but declined with the Revenue strategy. In addition N mineralization was much stronger with the Revenue scenario during elevated CO_2 period, with largest contribution from mineralization by microbial turnover.

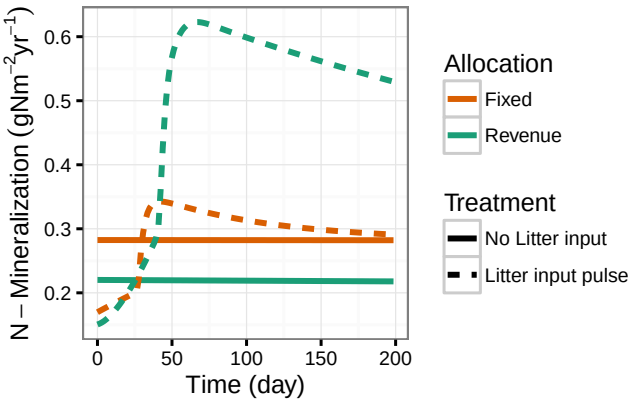

Figure 6. Priming a low-input soil by a fresh litter pulse stimulated N mineralization most strongly with the Revenue strategy with the Priming scenario.

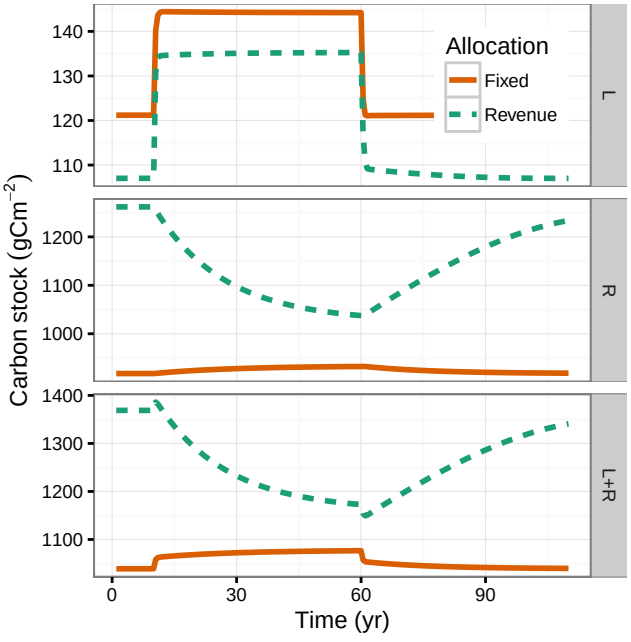

Figure 7. Revenue strategy led to a depletion of SOM, i.e. mining, during increased carbon litter inputs in years 10 to 60 with the CO_2-Fertilization scenario.

3.2 Intensive pasture simulation

The SEAM model successfully simulated the C and N balance of the Laqueuille intensive pasture (Figure 9 left). The observed continuous buildup of a pool of organic N in the residue SOM was driven by the systems positive N balance. It was simulated with SEAM by two pathways. First, inorganic N was taken up by the plant and supplied via organic N in litter, and second, microbial biomass immobilized inorganic N due to stoichiometric imbalance of substrate. The microbial

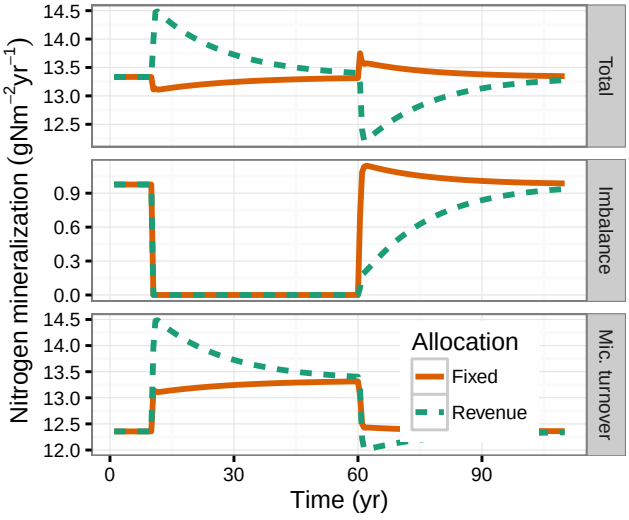

Figure 8. Mineralization of N associated with microbial turnover contributed most of the liberation of SOM-N with the Revenue strategy during CO_2-Fertilization, which started at year 10. At the end of the fertilization at year 60, mineralization asscociated with stoichiometric imbalance was smaller with the Revenue strategy.

biomass was N-limited when looking at the organic substrate only. However, it was C-limited when taking into account immobilization of inorganic N.

Alteration of C and N inputs to the system strongly affected the internal SOM and nutrient cycling. This effects was shown by several simulation scenarios that started from the calibrated state but applied a step change in inputs of litter or inorganic N (Figure 9 right) as detailed in following paragraphs.

Increased litter C input by 50% together with an increased litter C/N ratio by 25% with the elevated CO_2 scenario caused a shift in enzyme allocation towards enzymes degrading the N-rich residue pool and an increase of the litter pool. It also increased the demand for mineral N, both for the plant to balance increased biomass production and for microbial biomass with higher stoichiometric imbalance. The resulting decrease in mineral N also decreased leaching losses. In addition available N was reused more often, because of a higher turnover flux of N in increased microbial biomass.

Decreased inorganic N inputs from 22.9 $\mathrm{gm^{-2}yr^{-1}}$ down to 1 $\mathrm{gm^{-2}yr^{-1}}$ together with a doubling of litter C/N ratio caused a strong shift in enzyme allocation towards enzymes degrading the N-rich residue SOM with similar consequences as with increased C input, such as an increase in litter OM. However, here, the decreased N inputs caused a depletion of the mineral N pool. As a consequence, the microbial biomass could not use immobilization to balance substrate stoichiometry and became N-limited. This caused overflow respiration and a decreasing trend in residue SOM.

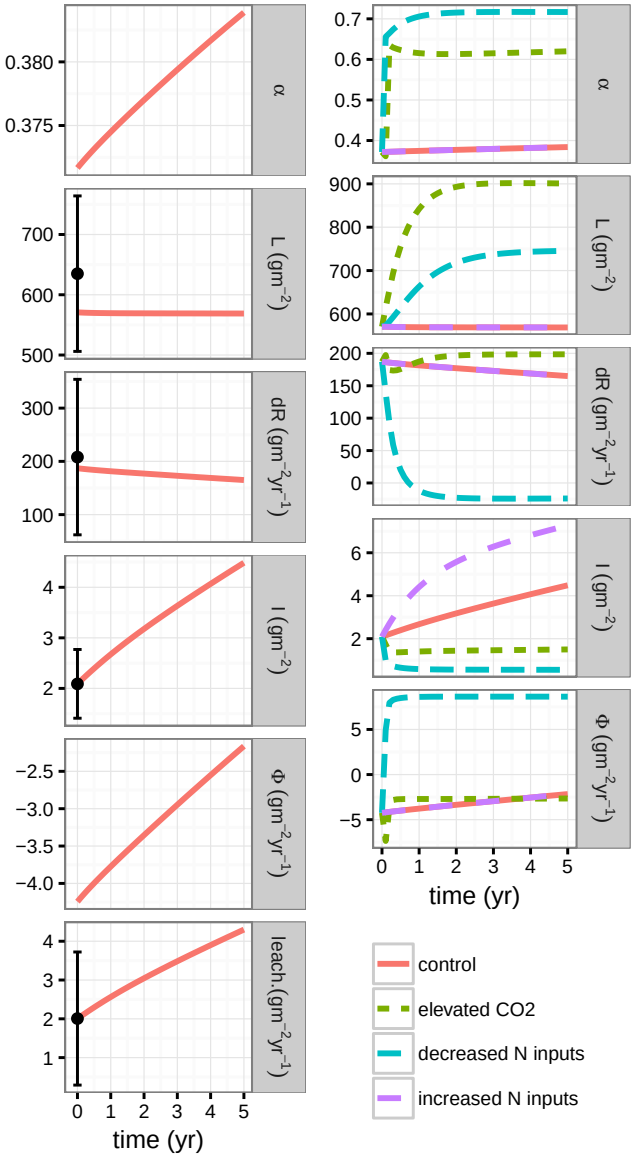

Figure 9. Calibrated Seam model predictions matched observed values of the Laqueuille intensive pasture (dots and errorbars left). Prescribed alteration of C and N inputs led to subsequent shifts in enzyme allocation (α) and affected development of soil pools (right) compared to the scenario of observed inputs (control same as in left panel). Increased N substrate limitation, either due to elevated CO_2 or due to decreasing inorganic N inputs, caused an increase in litter pool, L, and a decrease in mineral N pool, I. If the substrate N limitation could not be balanced by inorganic N input, then the change rate of the residue pool, dR, decreased down to negative values, i.e. losses.

Increased inorganic N inputs from 22.9 $\mathrm{gm^{-2}yr^{-1}}$ up to 25.6 $\mathrm{gm^{-2}yr^{-1}}$ together with a decrase of litter C/N by 25% did not much affect the system behaviour because the soil system was already C-limited before. The microbes could only immobilize a small part of the additional N for building up SOM. Instead, N accumulated in the inorganic pool with associated increased losses by leaching.

4 Discussion

Microbial adaptation of enzyme production benefited the community so that higher biomass levels could be sustained on a wider range of substrate stoichiometry. The different prototypic simulation scenarios and the simulation of the intensive pasture led to similar conclusions on comparing the different enzyme allocation adaptation strategies.

4.1 Amounts of resources matter

Both, the amounts of resource pools and resource stoichiometry are important for regulating enzyme allocation. The match strategy failed to account for resource amounts, assuming that microbes can achieve balanced growth under a wide range of resource stoichiometry (Moorhead et al., 2012; Ballantyne and Billings, 2014). The strategy was not competetive, as incidated by declining microbial biomass stocks both in the VarN-Incubation scenario (Fig. 3) and in the Sim-Steady scenarios (Fig. 4). Microbes focused on degrading a stoichiometrically balanced but declining residues pool despite the huge amount of N available in a large but stoichiometrically less favourable litter pool (Fig. 4). This finding implies that microbial enzyme allocation strategies must account for resource amounts.

4.2 Community adaptation leads to more efficient resource usage

The adaptive Revenue strategy consistently supported higher biomass and had lower N mineralization fluxes at steady state compared to the the non-adaptive Fixed strategy with the VarN-Incubation scenario (Fig. 3). Similar patterns appeared with the other scenarios (Figs. 4 and 8). Such better resource usage is in line with results of individual based small-scale modelling (Kaiser et al., 2014). The finding implies that N mineralization fluxes with imbalanced resources may be lower than inferred from previous modelling studies that did not account for community adaptation.

The SEAM model focuses on community adaptation of enzyme production. It predicts a change in the ratio of enzyme activities of enzymes degrading C-rich plant litter versus enzymes degrading the N-rich residue SOM when changing inputs of inorganic N to the soil. While low variation in stoichiometry of N-degrading versus C-degrading enzymatic activity is observed across biomes (Sinsabaugh et al., 2009), microcosm studies detect short-term changes of enzyme activities with N fertilization (Kumar et al., 2016), but their observations differ between different kinds of N-degrading enzymes. It implies that the simplifying assumptions of the

SEAM model are in line with more detailed models but cannot be directly compared and validated by observations yet.

4.3 SOM can store and release N

Nitrogen was stored in residue SOM during periods of high N inputs and released during periods of low N inputs relative to C inputs in simulations (Fig. 7). When there was excess litter carbon, microbial community preferentially depolymerized or mined the N rich residue pool and also made it available for plants by mineralization. Contrary, when there were low carbon inputs, microbes less strongly degraded the residue pool but continued to build it via microbial turnover. Hence, microbes kept N in the system instead of releasing it by mineralization. This bank mechanism (Perveen et al., 2014) also worked when simulating the intensive pasture (Fig. 9). During simulations of high inorganic N inputs, N was sequestered in SOM at a high rate. With decreased inorganic N inputs, the sequestration rate decreased until it became negative, i.e. the N in recalcitrat SOM was mined. Ultimately, on the long term, the inputs to the system have to balance the outputs of the system. In the intensive pasture simulation, inorganic N pools and N leaching increased with the increase of SOM with the SEAM model. This finding has consequences on feedbacks of global change, especially on the projected C land uptake (Friedlingstein et al., 2014). When accounting for the bank mechanisms land carbon sink and plant nutrition will not be as strongly N-limited.

4.4 Priming effects recycle N

Priming effects, i.e. the altered decomposition of SOM after soil amendmends (Kuzyakov et al., 2000), can help plants to stimulate N release for plant nutrition. Priming effects and associated increased N mineralization were simulated for all strategies (Fig. 5). With adaptive microbial enzyme allocation, plant litter inputs influenced the partitioning of SOM between a low and high C/N pools (Fig. 7) and, hence, also influenced the distribution of N in the ecosystem and nutrient availability for plants (Fig. 8). This active role of plant inputs has been demonstrated in a soil incubation experiment (Fontaine et al., 2011) and has been further conceptualized with the SYMPHONY model (Perveen et al., 2014). Our results are in line with these studies, although our explanation is on a more abstract level (section 4.6). The conservation or release of N by the bank mechanism implies greater potential for ecosystems to avoid progressive N limitation (Norby et al., 2010; Franklin et al., 2014; Averill et al., 2015).

Mineralization during microbial turnover is important for nutrient recycling. Without the additional mineralization mechanisms of uptake mineralization (Manzoni et al., 2008) and turnover mineralization (Clarholm, 1985; Raynaud et al., 2006) in our simulation experiment, microbes shifted enzyme allocation to degrade the residues pool, but the N was fixed in microbial biomass and was not mineralized to inorganic N. Hence, our experiments reinforced the need for representing soil heterogeneity and grazing for making N available for plants under N limitation.

4.5 Mismatch in time scale of priming effects

The unrealistically long time scale of priming effects in SEAM resulted from both, the turnover time of enzymes and the positive feedback between amounts of microbial biomass and enzymes. The time scale of priming effects of several month in SEAM simulations (Fig. 5) was in contrast with incubation studies that observe priming effects within days or weeks that rapidly declined after the amendmend has been used up (Blagodatskaya et al., 2014). Here, we discuss hypotheses of what processes could be reponsible for this mismatch and need further study. Priming timescale in SEAM was longer than the duration of the uptake pulse of the L amendment that only lasted a few days. It was controlled by simulated enzyme turnover, which SEAM described as first order kinetics with a turnover of about a week. Moreover, priming timescale was prolonged by the positive feedback of increased microbial biomass producing more enzymes that again fueled biomass.

One option to decrease priming timescale in SEAM is a different representation of enzyme turnover. Prescibing a shorter turnover time of enzymes, however, would require an increased effort of producing enzymes by microbial biomass. More sophisticated models of different enzyme turnover kinetics including stabilization of a part on mineral surfaces (Burns et al., 2013), hopefully, will be able to resolve such contradictions. Testing this hypothesis requires data on the fraction of uptake allocated to enzyme production and data on age distribution of enzymes in soil.

An alternative option to decrease priming timescale, is to describe the priming effect in a different manner. Some enzymes such as peroxidases need to be fueled by labile OM themselves (Rousk et al., 2014) with no immediate relationship to microbial biomass dynamics. This explanation, however, implies that enzyme activity and decomposition of SOM becomes decoupled from enzyme production and microbial dynamics to a large extent in the short term. This option is contrary to the assumption of most current models that simulate the priming effect.

Another option to decrease the priming timescale, is to diminish the sustaining positive feedback between enzymes and microbial biomass. Currently, grazing is an implicit part of a first order microbial turnover. With increasing microbial biomass, grazers become more efficient (Clarholm, 1981). With implementing a time-lagged stronger increase in microbial turnover rate with microbial biomass, biomass levels would decrease faster to pre-treatment levels and help to shorten the time-scale of the priming effect. Testing this hypothesis requires data on grazing during priming effects.

Overall, the unrealistically simulated priming time scale hints to gaps in understanding short-term SOM turnover.

However, it does not impair the simulated longer-term microbial community controls on SOM cycling. We argue that the simulated long-term patterns are robust, because they are more strongly controlled by the proportions in enzyme production than by the time scale of priming effects.

4.6 A holistic view for upscaling

The presented SEAM model takes a holistic view (Panikov, 2010) of microbial community and their adaptations instead of explicitely describing microbial diversity. In this respect, it differs from the SYMPHONY model (Perveen et al., 2014) and similar models (Fontaine et al., 2003), that explicitly modelled several microbial groups. The effective behaviour of the presented SEAM model, however, is similar. It assumes that community composition is driven to a large extent by external drivers. Specifically, it describes an adaptive allocation of resources into breakdown of different resources by assuming that the community composition adapts to changed resource availability in a way to optimize microbe's revenue. While the mechanistic approach of the SYMPHONY model explicitly represents this optimization by shifts between microbial groups, the holistic approach represents the effects of this optimization at community level. While the mechanistic approach gives more detailed understanding of the mechanism, we hypothesize, that the holistic approach is more suitable for upscaling (Wutzler and Reichstein, 2013). Hence, the proposed abstraction of microbial competition by the revenue strategy is a step forward of better representing couplings of soil carbon and nutrient cycles in earth system models and a step forward to improved predictions of long term carbon sequestration.

The holistic SEAM model yielded qualitatively similar predictions as the mechanistic SYMPHONY model with simulating priming, the bank mechanism, and a continuous SOM sequestration under high inorganic N inputs. It differed from SYMPHONY in the prediction of the inorganic N pool during low N inputs. Specifically, it predicted a decrease in this pool, while SYMPHONY predicted an increase in this pool due to changed competition (Perveen et al., 2014). The difference is probably caused by different assumptions on how the DOM pool is shared among groups of the microbial community and resulting different competition conditions. In the SEAM model, decomposition products become mixed in a shared DOM pool, while in the SYMPHONY model the decomposition products are not shared between the microbial groups. The truth at pore scale is in between, in that decomposition products are mainly used by the group that is producing the extracellular enzymes, while a part of the DOM diffuses also to other groups (Kaiser et al., 2014). At larger scales, such details cannot be measured or resolved. The difference in model prediction implies that the rationality of the simplified model assumptions of a mixed DOM pool can be qualitatively tested against observations.

4.7 Testable predictions of change of SOM C/N ratios

The SEAM model can be used to predict long term patterns of SOM cycling after changes in resource stoichiometry. Observations of such pattern provide evidence for or against the modelling assumptions. Specifically, SEAM predicted a change in proportions of the litter pool and the SOM pool (Fig. 7). While these abstract pools are not directly comparable to observations, a measureable consequence is the associated change of total SOM C/N ratio at the time scale of turnover of the residue pool. Specifically, SEAM predicted a decline in SOM stocks and an increase of SOM C/N with Face experiments at formerly C-limited systems over time scales of several decades.

4.8 Outlook

The biggest limitation of the SEAM model is its focus on a single process: community adaptation of enzyme allocation. In order to focus, we had to ignore several other important processes. One such process is the second microbial community strategy of handling resource stoichiometric imbalance, the adaption of stoichiometry of microbial biomass. Although the potential of this biomass adaptation is thought to be quite limited (Mooshammer et al., 2014b), it will be tested whether these two strategies can be combined within a model.

Next, the optimality principle will be extended to also determine the proportion of uptake that is allocated to enzyme production. Presence of cheaters, i.e. microbes that consume resource but without producing enzymes, effectively lower the community-level allocation to enzymes (Kaiser et al., 2014). Community development can be assumed to maximise biomass production. Such an assumption can be used to compute the optimal community enzyme production and allows exploring effects on SOM cycling, such as more constrained carbon and nutrient use efficiencies.

Moreover, SEAM will be simplified by assuming quasi-steady state of biomass or enzyme pools (Wutzler and Reichstein, 2013). These simplifications will lead to fewer parameters and improved identifiably in model calibration to observations. Togehter with implementing the influence of environmental factors such as temperature and moisture (Davidson et al., 2012), these changes will make SEAM more suitable to be used as a component within larger scale land surface models.

5 Conclusions

Adaptating resources allocation into the production of different enzymes is an effective means of the microbial community to react to changing resource stoichiometry. Allocation adaptation strategies helped microbial biomass in SEAM (Fig. 1) simulations to grow larger biomass across a wider range of resource stoichiometry (Fig. 3). Among the tested

strategies, the revenue strategy was particularly successful, which took into account both, the amount of resource and their stoichiometry. The findings imply that models that want to simulate soil carbon and nutrients dynamics (Figs. 5 and 6) must account for adaptations in carbon and nutrient strategies. Accounting for adaptations will be especially important, when studying the competition for nutrients between soil microorganism and plants, because SOM can function as a storage to sequester surplus elements and prevent them from leaving the system (Fig. 7 and 8).

The SEAM model provides a holistic description of community adaptations. It yields qualitatively similar predictions as microbial-group-explicit models with the ability to represent priming effects, bank mechanism, and a continuous SOM sequestration with high inorganic N inputs (Fig. 9).

Hence, this study provides an important step for providing an abstract description of microbial community effects and adaptations, with the long-term goal of including the important mechanisms into earth system models.

Appendix A: SEAM equations

A1 Carbon fluxes

$$\frac{dB}{dt} = \mathrm{syn}_B - \mathrm{tvr}_B \tag{A1a}$$
$$\frac{dE_L}{dt} = (1-\alpha)\,\mathrm{syn}_E - \mathrm{tvr}_{EL} \tag{A1b}$$
$$\frac{dE_R}{dt} = \alpha\,\mathrm{syn}_E - \mathrm{tvr}_{ER} \tag{A1c}$$
$$\frac{dL}{dt} = -\mathrm{dec}_L + \mathrm{input}_L \tag{A1d}$$
$$\frac{dR}{dt} = -\mathrm{dec}_R + \epsilon_{\mathrm{tvr}}\,\mathrm{tvr}_B + (1-k_{NB})(\mathrm{tvr}_{ER}+\mathrm{tvr}_{EL}), \tag{A1e}$$

where α is the proportion of total investment into enzymes that is allocated to the residue pool R (section 2.3), input_L is the litter C input to the system, ϵ_{tvr} is the fraction of microbial turnover C that is respired by predators, and k_{NB} is the fraction of enzyme turnover that is transferred to the DOM instead of the R pool. The specific fluxes are detailed below.

Total enzyme production syn_E, maintenance respiration r_M, and microbial turnover tvr_B are modelled as a first order kinetics of biomass:

$$\mathrm{syn}_E = a_E B \tag{A2a}$$
$$\mathrm{r}_M = mB \tag{A2b}$$
$$\mathrm{tvr}_B = \tau B \tag{A2c}$$

Enzyme turnover (tvr_{ER} and tvr_{EL}) is modelled as first order kinetics of enzyme levels.

$$\mathrm{tvr}_{ES} = k_{NS} E_S, \tag{A3}$$

where S represents either litter L or residue R substrate pools.

Substrate depolymerization is modelled first order to substrate availability with a saturating Michaelis-Menten kinetics to enzyme levels:

$$\mathrm{dec}_{S,Pot} = k_S S \tag{A4a}$$
$$\mathrm{dec}_S = dec_{S,Pot}\,\frac{E_S}{K_{M,S}+E_S} \tag{A4b}$$

The DOM pool is assumed to be in fast quasi steady state and all the sum of all influxes to the DOM pool (decomposition + part of the enzyme turnover) is taken up by microbial community.

$$u_C = \mathrm{dec}_L + \mathrm{dec}_R + k_{NB}(\mathrm{tvr}_{ER}+\mathrm{tvr}_{EL}) \tag{A5}$$

Under carbon limitation, carbon available for synthesis of new biomass and associated catabolic growth respiration, C_{synBC}, is the difference between carbon uptake and expenses for enzyme synthesis (eq. A2a) and maintenance respiration (eq. A2b).

$$C_{\mathrm{synBC}} = u_C - \mathrm{syn}_E/\epsilon - \mathrm{r}_M \tag{A6}$$

If carbon balance for biomass synthesis, syn_B (eq. A11), is positive, only a fraction ϵ, the anabolic carbon use efficiency, is used for synthesis of biomass and enzymes and the rest is required for catabolic growth respiration r_G to support this synthesis. The model assumes that requirements for enzyme synthesis and maintenance must be met. Hence, the balance could become negative where microbial biomass starves and declines.

$$\mathrm{syn}_B = \begin{cases} \epsilon C_{\mathrm{synB}}, & \text{if } C_{\mathrm{synB}} > 0 \\ C_{\mathrm{synB}}, & \text{otherwise} \end{cases} \tag{A7a}$$
$$\mathrm{r}_G = \begin{cases} (1-\epsilon)\,C_{\mathrm{synB}}, & \text{if } C_{\mathrm{synB}} > 0 \\ 0, & \text{otherwise}\ , \end{cases} \tag{A7b}$$

where C_{synB} is the carbon balance for biomass synthesis and is given below by eq. A11.

A2 Nitrogen fluxes

Nitrogen fluxes and pools are derived by dividing the respective fluxes with the C/N ratio, β, of their source.

The C/N ratios β_B and β_E of the microbial biomass and of the enzymes, are fixed. The C/N ratio of the litter pools, however, may change over time and the N pools are modelled explicitly.

$$\frac{dL_N}{dt} = -\mathrm{dec}_L/\beta_L + \mathrm{input}_L/\beta_\mathrm{i} \tag{A8a}$$
$$\frac{dR_N}{dt} = -\mathrm{dec}_R/\beta_R + \epsilon_{\mathrm{tvr}}\,\mathrm{tvr}_B/\beta_B + (1-k_{NB})(\mathrm{tvr}_{ER}+\mathrm{tvr}_{EL})/\beta_E \tag{A8b}$$
$$\frac{dI}{dt} = +i_I - k_{IP} - lI + \Phi \tag{A8c}$$
$$\Phi = \Phi_u + \Phi_B + \Phi_{\mathrm{tvr}} \tag{A8d}$$
$$\Phi_u = (1-\nu)u_{N,OM}, \tag{A8e}$$

where the balance of the inorganic nitrogen pool I sums inorganic inputs i_I, plant uptake k_{IP}, leaching lI, and the exchange flux with soil mirobial biomass, Φ. This exchange flux, here, is the sum of the apparent mineralization due to soil heterogeneity, Φ_u, mineralization-immobilization imbalance flux, Φ_B (A12c), and mineralization of a part of microbial turnover ,Φ_{tvr} (A14b), to compensate predator's stoichiometery for predator's respiration (section A5).

Organic N uptake, $u_{N,OM}$, was modelled as a PAR scheme, where apparantly part of the organic N that is taken up from DON is mineralized because of soil spots with high

N concentration in DOM (Manzoni et al., 2008). Potential nitrogen uptake is the sum of organic N uptake and the potential immobilization flux ($u_{\mathrm{imm,Pot}}$). Uptake from DOM is assumed equal to influxes to DOM times the apparent nitrogen use efficiency ν.

$$u_N = \nu u_{N,OM} + u_{\mathrm{imm,Pot}} \tag{A9a}$$

$$u_{N,OM} = \mathrm{dec}_L/\beta_L + \mathrm{dec}_R/\beta_R + k_{NB}(\mathrm{tvr}_{ER} + \mathrm{tvr}_{EL})/\beta_E \tag{A9b}$$

$$u_{\mathrm{imm,Pot}} = i_B I, \tag{A9c}$$

where C/N ratios β_L and β_R are calculated based on current C and N substrate pools: $\beta_L = L/L_N$.

The nitrogen available for biomass synthesis is the difference of nitrogen uptake and expenses for enzyme synthesis. This translates to a nitrogen constraint for the carbon used for biomass synthesis and its associated catabolic growth respiration: $C_{\mathrm{synB}} \leq C_{\mathrm{synBN}}$.

$$N_{\mathrm{synBN}} = u_N - \mathrm{syn}_E/\beta_E, \tag{A10a}$$

$$C_{\mathrm{synBN}} = \beta_B N_{\mathrm{synBN}}/\epsilon \tag{A10b}$$

A3 Imbalance fluxes of C versus N limited microbes

There are constraints of each element for the carbon flux for synthesis of new biomass and associated growth respiration. The minimum of these fluxes (eq. A11) constrains the synthesis of new biomass.

$$C_{\mathrm{synB}} = min(C_{\mathrm{synBC}}, C_{\mathrm{synBN}}) \tag{A11}$$

The excess elements are lost by imbalance fluxes (eq. A12). The excess carbon is respired by overflow respiration, r_O, and the excess nitrogen is mineralized, M_{Imb}, so that the mass balance is closed.

$$r_O = u_C - (\mathrm{syn}_B + \mathrm{syn}_E/\epsilon + \mathrm{r}_G + r_M) \tag{A12a}$$

$$M_{\mathrm{Imb}} = u_N - (\mathrm{syn}_B/\beta_B + \mathrm{syn}_E/\beta_E) \tag{A12b}$$

$$\Phi_B = M_{\mathrm{Imb}} - u_{\mathrm{imm,Pot}} \tag{A12c}$$

The real mineralization-immobilization flux Φ_B is the difference between potential immobilization and excess nitrogen mineralization. With carbon limitation this will be a positive mineralization flux. With substrate nitrogen limitation, this will be a negative flux corresponding to immobilization. With uptake nitrogen limitation, i.e. required immobilization is larger than potential immobilization, $\Phi_B = -u_{\mathrm{imm,Pot}}$ and stoichiometry must be balanced by overflow respiration.

A4 Weight of an element limitation

The weight of an element limitation is computed as the ratio between required uptake flux for given other constraints to the available fluxes for biosynthesis.

$$w_{\mathrm{CLim}} = \left(\frac{\text{required}}{\text{available}}\right)^{\delta} = \left(\frac{N_{\mathrm{synBN}}\beta_B}{C_{\mathrm{synBC}}}\right)^{\delta} \tag{A13a}$$

$$w_{\mathrm{NLim}} = \left(\frac{C_{\mathrm{synBC}}/\beta_B}{N_{\mathrm{synBN}}}\right)^{\delta}, \tag{A13b}$$

where parameter δ, which was arbitrarily set to 200, controls the steepness of the transition between the two limitations. X_{synBY} denotes the available flux of element X for biosynthesis and associated respiration given the limitation of element Y (A6) and (A10).

A5 Turnover mineralization fluxes

In addition to mineralization flux due to stoichiometric imbalance, a part of microbial biomass is mineralized during microbial turnover, e.g. by grazing. A part $(1-\epsilon_{\mathrm{tvr}})$ of the biomass is used for catabolic respiration. With assuming that predator biomass elemental ratios do not differ very much from the one of microbial biomass, a respective proportion of N must be mineralized.

$$r_{\mathrm{tvr}} = (1-\epsilon_{\mathrm{tvr}})\,\mathrm{tvr}_B \tag{A14a}$$

$$\Phi_{\mathrm{tvr}} = (1-\epsilon_{\mathrm{tvr}})\,\mathrm{tvr}_B/\beta_B \tag{A14b}$$

All the non-respired turnover C enters the residue pool. In reality, a part of the microbial turnover probably enters the DOM pool again (e.g. by cell lysis) and is taken up again by microbial biomass. The increased uptake nearly cancels with an increased turnover. Hence, SEAM does not explicitly consider this shortcut loop so that fewer model parameters are required. Note, however, that turnover, uptake, and carbon use efficiency in the model are slightly lower than in the real system where this shortcut operates.

Appendix B: Allocation partitioning that matches microbial stoichiometry

The following equation was derived by solving (2) for allocation partitioning coefficient α using SymPy (SymPy Development Team, 2016). The sympy script and the R function evaluating the expression are provided as electronic supplements.

$$
\begin{aligned}
\alpha_M = -(&-E^2\beta_L\beta_B\beta_R\Phi_M - \\
&E^2\beta_L\beta_B\,\mathrm{dec}_{R,Pot} + E^2\beta_L\beta_R\,\mathrm{dec}_{L,Pot}\,\epsilon + \\
&E^2\beta_L\beta_R\,\mathrm{dec}_{R,Pot}\,\epsilon - E^2\beta_L\beta_R\epsilon r_M - \\
&E^2\beta_B\beta_R\,\mathrm{dec}_{L,Pot} - E\beta_L\beta_B\,\mathrm{dec}_{R,Pot}\,K_{M,R} - \\
&E\beta_L\beta_R\,\mathrm{dec}_{L,Pot}\,\epsilon K_{M,R} + E\beta_L\beta_R\,\mathrm{dec}_{R,Pot}\,\epsilon K_{M,R} + \\
&E\beta_B\beta_R\,\mathrm{dec}_{L,Pot}\,K_{M,R} + sqrt(E^2\beta_L^2\beta_B^2\beta_R^2\Phi_M^2 + \\
&2E^2\beta_L^2\beta_B^2\beta_R\,\mathrm{dec}_{R,Pot}\,\Phi_M + \\
&E^2\beta_L^2\beta_B^2\,\mathrm{dec}_{R,Pot}^2 - 2E^2\beta_L^2\beta_B\beta_R^2\,\mathrm{dec}_{L,Pot}\,\epsilon\Phi_M - \\
&2E^2\beta_L^2\beta_B\beta_R^2\,\mathrm{dec}_{R,Pot}\,\epsilon\Phi_M + 2E^2\beta_L^2\beta_B\beta_R^2\epsilon\Phi_M r_M - \\
&2E^2\beta_L^2\beta_B\beta_R\,\mathrm{dec}_{L,Pot}\,\mathrm{dec}_{R,Pot}\,\epsilon - \\
&2E^2\beta_L^2\beta_B\beta_R\,\mathrm{dec}_{R,Pot}^2\,\epsilon + 2E^2\beta_L^2\beta_B\beta_R\,\mathrm{dec}_{R,Pot}\,\epsilon r_M + \\
&E^2\beta_L^2\beta_R^2\,\mathrm{dec}_{L,Pot}^2\,\epsilon^2 + 2E^2\beta_L^2\beta_R^2\,\mathrm{dec}_{L,Pot}\,\mathrm{dec}_{R,Pot}\,\epsilon^2 - \\
&2E^2\beta_L^2\beta_R^2\,\mathrm{dec}_{L,Pot}\,\epsilon^2 r_M + E^2\beta_L^2\beta_R^2\,\mathrm{dec}_{R,Pot}^2\,\epsilon^2 - \\
&2E^2\beta_L^2\beta_R^2\,\mathrm{dec}_{R,Pot}\,\epsilon^2 r_M + E^2\beta_L^2\beta_R^2\epsilon^2 r_M^2 + \\
&2E^2\beta_L\beta_B^2\beta_R^2\,\mathrm{dec}_{L,Pot}\,\Phi_M + \\
&2E^2\beta_L\beta_B^2\beta_R\,\mathrm{dec}_{L,Pot}\,\mathrm{dec}_{R,Pot} - 2E^2\beta_L\beta_B\beta_R^2\,\mathrm{dec}_{L,Pot}^2\,\epsilon - \\
&2E^2\beta_L\beta_B\beta_R^2\,\mathrm{dec}_{L,Pot}\,\mathrm{dec}_{R,Pot}\,\epsilon + \\
&2E^2\beta_L\beta_B\beta_R^2\,\mathrm{dec}_{L,Pot}\,\epsilon r_M + \\
&E^2\beta_B^2\beta_R^2\,\mathrm{dec}_{L,Pot}^2 + 4E\beta_L^2\beta_B^2\beta_R^2\Phi_M^2 K_{M,R} + \\
&6E\beta_L^2\beta_B^2\beta_R\,\mathrm{dec}_{R,Pot}\,\Phi_M K_{M,R} + \\
&2E\beta_L^2\beta_B^2\,\mathrm{dec}_{R,Pot}^2\,K_{M,R} - 6E\beta_L^2\beta_B\beta_R^2\,\mathrm{dec}_{L,Pot}\,\epsilon\Phi_M K_{M,R} - \\
&6E\beta_L^2\beta_B\beta_R^2\,\mathrm{dec}_{R,Pot}\,\epsilon\Phi_M K_{M,R} + \\
&8E\beta_L^2\beta_B\beta_R^2\epsilon\Phi_M K_{M,R} r_M - \\
&4E\beta_L^2\beta_B\beta_R\,\mathrm{dec}_{L,Pot}\,\mathrm{dec}_{R,Pot}\,\epsilon K_{M,R} - \\
&4E\beta_L^2\beta_B\beta_R\,\mathrm{dec}_{R,Pot}^2\,\epsilon K_{M,R} + \\
&6E\beta_L^2\beta_B\beta_R\,\mathrm{dec}_{R,Pot}\,\epsilon K_{M,R} r_M + \\
&2E\beta_L^2\beta_R^2\,\mathrm{dec}_{L,Pot}^2\,\epsilon^2 K_{M,R} + \\
&4E\beta_L^2\beta_R^2\,\mathrm{dec}_{L,Pot}\,\mathrm{dec}_{R,Pot}\,\epsilon^2 K_{M,R} - \\
&6E\beta_L^2\beta_R^2\,\mathrm{dec}_{L,Pot}\,\epsilon^2 K_{M,R} r_M + \\
&2E\beta_L^2\beta_R^2\,\mathrm{dec}_{R,Pot}^2\,\epsilon^2 K_{M,R} - \\
&6E\beta_L^2\beta_R^2\,\mathrm{dec}_{R,Pot}\,\epsilon^2 K_{M,R} r_M + 4E\beta_L^2\beta_R^2\epsilon^2 K_{M,R} r_M^2 + \\
&6E\beta_L\beta_B^2\beta_R^2\,\mathrm{dec}_{L,Pot}\,\Phi_M K_{M,R} + \\
&4E\beta_L\beta_B^2\beta_R\,\mathrm{dec}_{L,Pot}\,\mathrm{dec}_{R,Pot}\,K_{M,R} - \\
&4E\beta_L\beta_B\beta_R^2\,\mathrm{dec}_{L,Pot}^2\,\epsilon K_{M,R} - \\
&4E\beta_L\beta_B\beta_R^2\,\mathrm{dec}_{L,Pot}\,\mathrm{dec}_{R,Pot}\,\epsilon K_{M,R} + \\
&6E\beta_L\beta_B\beta_R^2\,\mathrm{dec}_{L,Pot}\,\epsilon K_{M,R} r_M + \\
&2E\beta_B^2\beta_R^2\,\mathrm{dec}_{L,Pot}^2\,K_{M,R} + 4\beta_L^2\beta_B^2\beta_R^2\Phi_M^2 K_{M,R}^2 + \\
&4\beta_L^2\beta_B^2\beta_R\,\mathrm{dec}_{R,Pot}\,\Phi_M K_{M,R}^2 + \beta_L^2\beta_B^2\,\mathrm{dec}_{R,Pot}^2\,K_{M,R}^2 - \\
&4\beta_L^2\beta_B\beta_R^2\,\mathrm{dec}_{L,Pot}\,\epsilon\Phi_M K_{M,R}^2 - \\
&4\beta_L^2\beta_B\beta_R^2\,\mathrm{dec}_{R,Pot}\,\epsilon\Phi_M K_{M,R}^2 + 8\beta_L^2\beta_B\beta_R^2\epsilon\Phi_M K_{M,R}^2 r_M + \\
&2\beta_L^2\beta_B\beta_R\,\mathrm{dec}_{L,Pot}\,\mathrm{dec}_{R,Pot}\,\epsilon K_{M,R}^2 - \\
&2\beta_L^2\beta_B\beta_R\,\mathrm{dec}_{R,Pot}^2\,\epsilon K_{M,R}^2 + \\
&4\beta_L^2\beta_B\beta_R\,\mathrm{dec}_{R,Pot}\,\epsilon K_{M,R}^2 r_M + \beta_L^2\beta_R^2\,\mathrm{dec}_{L,Pot}^2\,\epsilon^2 K_{M,R}^2 - \\
&2\beta_L^2\beta_R^2\,\mathrm{dec}_{L,Pot}\,\mathrm{dec}_{R,Pot}\,\epsilon^2 K_{M,R}^2 - \\
&4\beta_L^2\beta_R^2\,\mathrm{dec}_{L,Pot}\,\epsilon^2 K_{M,R}^2 r_M + \beta_L^2\beta_R^2\,\mathrm{dec}_{R,Pot}^2\,\epsilon^2 K_{M,R}^2 - \\
&4\beta_L^2\beta_R^2\,\mathrm{dec}_{R,Pot}\,\epsilon^2 K_{M,R}^2 r_M + 4\beta_L^2\beta_R^2\epsilon^2 K_{M,R}^2 r_M^2 + \\
&4\beta_L\beta_B^2\beta_R^2\,\Phi_M K_{M,R}^2 - \\
&2\beta_L\beta_B^2\beta_R\,\mathrm{dec}_{L,Pot}\,\mathrm{dec}_{R,Pot}\,K_{M,R}^2 - \\
&2\beta_L\beta_B\beta_R^2\,\mathrm{dec}_{L,Pot}^2\,\epsilon K_{M,R}^2 + \\
&2\beta_L\beta_B\beta_R^2\,\mathrm{dec}_{L,Pot}\,\mathrm{dec}_{R,Pot}\,\epsilon K_{M,R}^2 + \\
&4\beta_L\beta_B\beta_R^2\,\mathrm{dec}_{L,Pot}\,\epsilon K_{M,R}^2 r_M + \\
&\beta_B^2\beta_R^2\,\mathrm{dec}_{L,Pot}^2\,K_{M,R}^2)abs(E))/(2E^2\beta_L\beta_B\beta_R\Phi_M + \\
&2E^2\beta_L\beta_B\,\mathrm{dec}_{R,Pot} - 2E^2\beta_L\beta_R\,\mathrm{dec}_{L,Pot}\,\epsilon - \\
&2E^2\beta_L\beta_R\,\mathrm{dec}_{R,Pot}\,\epsilon + 2E^2\beta_L\beta_R\epsilon r_M + \\
&2E^2\beta_B\beta_R\,\mathrm{dec}_{L,Pot}),
\end{aligned}
$$

where $E = E_R + E_L$

Acknowledgements. We thank Nazia Perveen and Sébastien Fontaine for letting us reuse the data that they used for fitting the SYMPHONY model.

References

Allard, V., Soussana, J.-F., Falcimagne, R., Berbigier, P., Bonnefond, J., Ceschia, E., D'hour, P., Hénault, C., Laville, P., Martin, C., and Pinarès-Patino, C.: The role of grazing management for the net biome productivity and greenhouse gas budget (CO2, {N2O} and CH4) of semi-natural grassland, Agriculture, Ecosystems & Environment, 121, 47 – 58, doi:http://dx.doi.org/10.1016/j.agee.2006.12.004, 2007.

Allison, S. D.: Modeling adaptation of carbon use efficiency in microbial communities, Frontiers in Microbiology, 5, doi:10.3389/fmicb.2014.00571, 2014.

Allison, S. D. and Vitousek, P. M.: Responses of extracellular enzymes to simple and complex nutrient inputs, Soil Biology & Biochemistry, 37, 937–944, 2005.

Averill, C., Rousk, J., and Hawkes, C.: Microbial-mediated redistribution of ecosystem nitrogen cycling can delay progressive nitrogen limitation, Biogeochemistry, 126, 11–23, doi:10.1007/s10533-015-0160-x, 2015.

Ballantyne, F. and Billings, S.: Shifting resource availability, plastic allocation to exoenzymes and the consequences for heterotrophic soil respiration, in: EGU General Assembly Conference Abstracts, vol. 16 of *EGU General Assembly Conference Abstracts*, p. 16780, http://adsabs.harvard.edu/abs/2014EGUGA..16167 80B, 2014.

Blagodatskaya, E., Khomyakov, N., Myachina, O., Bogomolova, I., Blagodatsky, S., and Kuzyakov, Y.: Microbial interactions affect sources of priming induced by cellulose, Soil Biology and Biochemistry, 74, 39–49, doi:10.1016/j.soilbio.2014.02.017, 2014.

Burns, R. G., DeForest, J. L., Marxsen, J., Sinsabaugh, R. L., Stromberger, M. E., Wallenstein, M. D., Weintraub, M. N., and Zoppini, A.: Soil enzymes in a changing environment: Current knowledge and future directions, Soil Biology and Biochemistry, 58, 216 – 234, doi:10.1016/j.soilbio.2012.11.009, 2013.

Clarholm, M.: Protozoan grazing of bacteria in soil - impact and importance, Microbial Ecology, 7, 343–350, doi:10.1007/bf02341429, 1981.

Clarholm, M.: Interactions of bacteria, protozoa and plants leading to mineralization of soil nitrogen, Soil Biology and Biochemistry, 17, 181–187, doi:10.1016/0038-0717(85)90113-0, 1985.

Cleveland, C. C. and Liptzin, D.: C:N:P stoichiometry in soil: is there a Redfield ratio for the microbial biomass?, Biogeochemistry, 85, 235–252, doi:10.1007/s10533-007-9132-0, 2007.

Davidson, E. A., Samanta, S., Caramori, S. S., and Savage, K.: The Dual Arrhenius and Michaelis–Menten kinetics model for decomposition of soil organic matter at hourly to seasonal time scales, Global Change Biology, 18, 371–384, doi:10.1111/j.1365-2486.2011.02546.x, 2012.

Fontaine, S., Mariotti, A., and Abbadie, L.: The priming effect of organic matter: a question of microbial competition?, Soil Biology & Biochemistry, 35, 837–843, 2003.

Fontaine, S., Henault, C., Aamor, A., Bdioui, N., Bloor, J., Maire, V., Mary, B., Revaillot, S., and Maron, P.: Fungi mediate long term sequestration of carbon and nitrogen in soil through their priming effect, Soil Biology and Biochemistry, 43, 86–96, doi:10.1016/j.soilbio.2010.09.017, 2011.

Franklin, O., Näsholm, T., Högberg, P., and Högberg, M. N.: Forests trapped in nitrogen limitation - an ecological market perspective on ectomycorrhizal symbiosis, New Phytol, 203, 657–666, doi:10.1111/nph.12840, 2014.

Friedlingstein, P., Meinshausen, M., Arora, V. K., Jones, C. D., Anav, A., Liddicoat, S. K., and Knutti, R.: Uncertainties in CMIP5 climate projections due to carbon cycle feedbacks, Journal of Climate, 27, 511–526, doi:10.1175/JCLI-D-12-00579.1, 2014.

Janssens, I. A., Dieleman, W., Luyssaert, S., Subke, J.-A., Reichstein, M., Ceulemans, R., Ciais, P., Dolman, A. J., Grace, J., Matteucci, G., and et al.: Reduction of forest soil respiration in response to nitrogen deposition, Nature Geosci, 3, 315–322, doi:10.1038/ngeo844, 2010.

Kaiser, C., Franklin, O., Dieckmann, U., and Richter, A.: Microbial community dynamics alleviate stoichiometric constraints during litter decay, Ecol Lett, 17, 680–690, doi:10.1111/ele.12269, 2014.

Kumar, A., Kuzyakov, Y., and Pausch, J.: Maize rhizosphere priming: field estimates using 13C natural abundance, Plant and Soil, doi:10.1007/s11104-016-2958-2, 2016.

Kuzyakov, Y., Friedel, J. K., and Stahr, K.: Review of mechanisms and quantification of priming effects, Soil Biology & Biochemistry, 32, 1485–1498, 2000.

Manzoni, S. and Porporato, A.: Soil carbon and nitrogen mineralization: Theory and models across scales, Soil Biology and Biochemistry, 41, 1355–1379, doi:10.1016/j.soilbio.2009.02.031, 2009.

Manzoni, S., Porporato, A., and Schimel, J. P.: Soil heterogeneity in lumped mineralization-immobilization models, Soil Biology & Biochemistry, 40, 1137–1148, doi:10.1016/j.soilbio.2007.12.006, 2008.

Moorhead, D. L., Lashermes, G., and Sinsabaugh, R. L.: A theoretical model of C-and N-acquiring exoenzyme activities, which balances microbial demands during decomposition, Soil Biology and Biochemistry, 53, 133–141, doi:10.1016/j.soilbio.2012.05.011, 2012.

Mooshammer, M., Wanek, W., Hämmerle, I., Fuchslueger, L., Hofhansl, F., Knoltsch, A., Schnecker, J., Takriti, M., Watzka, M., Wild, B., and et al.: Adjustment of microbial nitrogen use efficiency to carbon:nitrogen imbalances regulates soil nitrogen cycling, Nat Comms, 5, doi:10.1038/ncomms4694, 2014a.

Mooshammer, M., Wanek, W., Zechmeister-Boltenstern, S., and Richter, A.: Stoichiometric imbalances between terrestrial decomposer communities and their resources: mechanisms and implications of microbial adaptations to their resources, Frontiers in Microbiology, 5, doi:10.3389/fmicb.2014.00022, 2014b.

Norby, R. J., Warren, J. M., Iversen, C. M., Medlyn, B. E., and McMurtrie, R. E.: CO2 enhancement of forest productivity constrained by limited nitrogen availability, Proceedings of the National Academy of Sciences, 107, 19 368–19 373, doi:10.1073/pnas.1006463107, 2010.

Panikov, N. S.: Microbial Ecology, Environmental Biotechnology, pp. 121–191, doi:10.1007/978-1-60327-140-0_4, 2010.

Perveen, N., Barot, S., Alvarez, G., Klumpp, K., Martin, R., Rapaport, A., Herfurth, D., Louault, F., and Fontaine, S.: Priming effect and microbial diversity in ecosystem functioning

and response to global change: a modeling approach using the SYMPHONY model, Glob Change Biol, 20, 1174 – 1190, doi:10.1111/gcb.12493, 2014.

R Core Team: R: A Language and Environment for Statistical Computing, R Foundation for Statistical Computing, Vienna, Austria, https://www.R-project.org, 2016.

Rastetter, E. B.: Modeling coupled biogeochemical cycles, Frontiers in Ecology and the Environment, 9, 68 – 73, doi:10.1890/090223, 2011.

Rastetter, E. B., Ågren, G. I., and Shaver, G. R.: RESPONSES OF N-LIMITED ECOSYSTEMS TO INCREASED CO2: A BALANCED-NUTRITION, COUPLED-ELEMENT-CYCLES MODEL, Ecological Applications, 7, 444–460, doi:10.1890/1051-0761(1997)007[0444:RONLET]2.0.CO;2, 1997.

Raynaud, X., Lata, J. C., and Leadley, P. W.: Soil microbial loop and nutrient uptake by plants: a test using a coupled C : N model of plant-microbial interactions, Plant and Soil, 287, 95–116, doi:10.1007/s11104-006-9003-9, 2006.

Resat, H., Bailey, V., McCue, L. A., and Konopka, A.: Modeling Microbial Dynamics in Heterogeneous Environments: Growth on Soil Carbon Sources, Microbial Ecology, 63, 883–897, doi:10.1007/s00248-011-9965-x, 2011.

Rousk, J., Hill, P. W., and Jones, D. L.: Priming of the decomposition of ageing soil organic matter: concentration dependence and microbial control, Functional Ecology, 29, 285–296, doi:10.1111/1365-2435.12377, 2014.

Schimel, J. P. and Weintraub, M. N.: The implications of exoenzyme activity on microbial carbon and nitrogen limitation in soil: a theoretical model, Soil Biology and Biochemistry, 35, 549–563, 2003.

Sinsabaugh, R. L., Hill, B. H., and Follstad Shah, J. J.: Ecoenzymatic stoichiometry of microbial organic nutrient acquisition in soil and sediment, Nature, 462, 795–798, doi:10.1038/nature08632, 2009.

Sinsabaugh, R. L., Manzoni, S., Moorhead, D. L., and Richter, A.: Carbon use efficiency of microbial communities: stoichiometry, methodology and modelling, Ecology Letters, 16, 930–939, doi:10.1111/ele.12113, 2013.

Sterner, R. W. and Elser, J. J.: Ecological stoichiometry: the biology of elements from molecules to the biosphere, Princeton University Press, 2002.

SymPy Development Team: SymPy: Python library for symbolic mathematics, http://www.sympy.org, 2016.

Thornton, P. E., Lamarque, J.-F., Rosenbloom, N. A., and Mahowald, N. M.: Influence of carbon-nitrogen cycle coupling on land model response to CO 2 fertilization and climate variability, Global Biogeochemical Cycles, 21, doi:10.1029/2006gb002868, 2007.

van Bodegom, P.: Microbial maintenance: A critical review on its quantification, Microbial Ecology, 53, 513–523, 2007.

Wang, G., Post, W. M., and Mayes, M. A.: Development of microbial-enzyme-mediated decomposition model parameters through steady-state and dynamic analyses, Ecological Applications, 23, 255–272, doi:10.1890/12-0681.1, 2013.

Wieder, W. R., Bonan, G. B., and Allison, S. D.: Global soil carbon projections are improved by modelling microbial processes, Nature Climate Change, doi:10.1038/nclimate1951, 2013.

Wutzler, T. and Reichstein, M.: Colimitation of decomposition by substrate and decomposers - a comparison of model formulations, Biogeosciences, 5, 749–759, doi:10.5194/bg-5-749-2008, 2008.

Wutzler, T. and Reichstein, M.: Priming and substrate quality interactions in soil organic matter models, Biogeosciences, 10, 2089–2103, doi:10.5194/bg-10-2089-2013, 2013.

Xu, X., Thornton, P. E., and Post, W. M.: A global analysis of soil microbial biomass carbon, nitrogen and phosphorus in terrestrial ecosystems, Global Ecology and Biogeography, 22, 737–749, doi:10.1111/geb.12029, 2013.

Zaehle, S. and Dalmonech, D.: Carbon-nitrogen interactions on land at global scales: current understanding in modelling climate biosphere feedbacks, Current Opinion in Environmental Sustainability, 3, 311–320, doi:10.1016/j.cosust.2011.08.008, 2011.

Zechmeister-Boltenstern, S., Keiblinger, K. M., Mooshammer, M., Penuelas, J., Richter, A., Sardans, J., and Wanek, W.: The application of ecological stoichiometry to plant - microbial - soil organic matter transformations, Ecological Monographs, 85, 133–155, doi:10.1890/14-0777.1, 2015.